Journal of Metals, Materials and Minerals, Vol. 31, No. 4, pp. 45-50, 2021

Oxidation behavior of Sn-1 wt% Bi alloy in air and deionized water at room temperature

Tanavut NARAVUTHICHAI[1], Benjie FERNANDEZ[2], Ittipon CHEOWANISH[2], Patama VISUTTIPITUKUL[1], Sirichai LEELACHAO[1,*], and Tachai LUANGVARANUNT[1]

[1] *Department of Metallurgical Engineering, Faculty of Engineering, Chulalongkorn University, Phayathai Road, Bangkok, 10330, Thailand*
[2] *Department of Slider Development, Thailand Head Operation, Western Digital Storage Technologies (Thailand) Ltd., 140 Moo 2, Udomsorayuth Road, Bangpa-In Ayutthaya 13160, Thailand*

***Corresponding author e-mail:** endis@upi.edu

Received date:
8 May 2021
Revised date
24 August 2021
Accepted date:
26 August 2021

Keywords:
Electrochemical analysis;
Oxidation of tin;
Thickness of tin oxide film;
X-ray photoelectron spectroscopy

Abstract

Formation of tin oxides on surface Sn-1 wt% Bi alloy lapping plates causes interactions with protrusions of embedded diamond grits, and reduces the efficiency of the lapping process. The rate and type of oxide formation were investigated to understand the problem. Electrochemical analysis was performed to characterize the oxide film thickness, and x-ray photoelectron spectroscopy was performed to characterize the tin oxide species. Oxidation in air at room temperature reaches a thickness of 23 Å after 72 h. Oxidation in deionized water at room temperature has a faster growth rate, and reaches a thickness of 33 Å after 72 h. An oxides formation model is proposed for this tin alloy composition. The first layer is either a very thin layer or comprises clusters of SnO_2. The second layer is a thick and continuous SnO layer. The third layer is a mixture of the two types of oxides. Oxidation either in air or in deionized water at room temperature starts with a linear growth law, and changes to a parabolic growth law after the SnO layer reaches a critical thickness. There is a possibility of SnO to SnO_2 transformation that causes thickness reduction.

1. Introduction

The surface of a hard disk read-write head requires an extremely low surface roughness in order to function properly. The lapping process, being one of the final surface preparation steps, is carried out using an Sn-1 wt% Bi alloy lapping plate charged with nanosized diamond grits. Variation of lapping rate are always observed in lapping operation, and impact on the efficiency of the lapping process. The relationship between the lapping rate and the aging time in-storage was observed. The oxide film thickness of Sn-1 wt% Bi alloy is suspected to be the cause, and needs to be understood. Oxidation of tin lapping plate occurs continuously in all stages of a service cycle: i) in-use, ii) in-reconditioning stages under wet conditions, and iii) in-storage stage under ambient air. Classically, the thickness of any oxide films increases with time in a parabolic character, reaching a constant thickness at a long exposure time. In the case of oxide film on lapping plate, the film may continuously grow until it entirely covers the embedded diamond grits on the surface. For the oxide synthesized by thermal process [1,2], although an oxidation phenomenon has been examined, however, a film thickness measurement was not conducted.

The Sequential Electrochemical Reduction Analysis (SERA) technique is one of several methods that can be used to measure the thickness of tin oxide film. It has many advantages, such as being convenient to set up, giving a quick result, and being a non-destructive and inexpensive method. Many researchers have verified that this technique gives a measured value comparable to those of other techniques [3,4]. The SERA technique involves the application of a small constant cathodic current via an inert counter electrode to the test sample in a deaerated electrolyte. The optimal value of the applied current for the tin sample is between -30 μA and -100 μA [5-7]. A plot of cathode voltage versus time, called a chronopotentiogram, shows a series of plateaus corresponding to sequential reduction of the oxides present on the surface of the sample. A plateau voltage reflects the bonding strength of the oxide. The reduction time, which correlates to amount of reduction in the charge, is a measure of the amount of oxide being reduced [3-9]. There are two types of tin oxide film that are commonly found; they are SnO (Tin(II)oxide, stannous oxide) and SnO_2 (Tin(IV)oxide, stannic oxide) [5-10]. X-ray photoelectron spectroscopy (XPS) with ion gun sputtering can be used to confirm the correct species of tin oxide in each film layer [6,11-13].

The purpose of this research work is to study the growth rate of tin oxide film, which occurs on the surface of tin lapping plate under room temperature in air and in deionized water. The goal is to simulate the in-use, in-reconditioning, and in-storage stages in actual lapping operation. Both thickness and types of oxide layer will be measured and characterized.

2. Experimental

2.1 Material

Tin lapping plates were obtained from Western Digital (Thailand) Co., Ltd. The composition was 99.0 wt% Sn and 1.0 wt% Bi. The dimensions of tin test samples were 20 × 20 × 2 mm^3. The surface of

each sample was polished with 400, 600, 800 and 1000 grit SiC paper respectively, before annealed at 200°C for 1 h. After annealing, the sample was polished again with 1000 grit SiC paper, and washed with deionized water and acetone.

2.2 Oxidation test

The first oxidation test condition was in an air-conditioned room having a temperature range of between 24.7°C and 27.6°C, with 30% to 32% relative humidity. The second oxidation test condition was in deionized water in the same air-conditioned room. All samples were oxidized for 1, 2, 4, 24, 48, and 72 h.

2.3 Sequential Electrochemical Reduction Analysis (SERA)

A galvanostat (Autolab B.V., model PGSTAT204) was used to measure thickness of tin oxide film on the samples in each SERA experiment. The experiments were performed in a borate buffer solution (6.18 $g{\cdot}L^{-1}$ boric acid and 9.55 $g{\cdot}L^{-1}$ sodium tetraborate decahydrate) at a pH 8.4 [5-7], under argon atmosphere. An electrochemical flat cell has separate compartments for a platinum rod counter electrode, Ag/AgCl reference electrode, and a glass tube to purge argon gas, as shown in Figure 1. A reduction current of -40 µA was employed in all tests.

2.4 X-ray photoelectron spectroscopy (XPS)

XPS was carried out using Kratos Axis Ultra DLD, by Al Kα radiation. Each specimen was examined (i) before argon ion etching, and after argon ion etching for (ii) 10 s with 500 eV for 10 cycles, (iii) 10 s with 1 keV for 10 cycles, and (iv) 10 s with 3 keV for 10 cycles, respectively.

3. Results and discussion

3.1 Thickness of oxide film

Figure 2 shows SERA curves obtained from oxidation of tin in air at room temperature for 72 h. It can serve as the representative of Sn-1 wt% Bi oxidation behavior. It reveals reduction of tin oxides, which can be separated into three zones of reduction. Firstly, in zone 1, the initial potential drop at the very beginning is believed by many researchers to be the reduction of clusters of oxides at the outer surface, and discontinuity or minuscule defects on surface [6,7,14,15]. Due to the non-uniform nature of this outermost oxide layer, there is no reduction plateau with constant potential in the graph at this point. After the clusters of oxide film are removed, the next layer of oxide film is revealed by the first plateau in zone 1. This layer is quite dense and continuous, which is reflected in the obtained smooth plateau having an almost constant reduction potential. Reduction in zone 2 appears after the oxide layer in zone 1 is removed. The plateau in zone 2 is not as well-defined as that in zone 1.

The first plateau in zone 1 is SnO [5-9]. Some previous research [5-9] has identified the not well-defined plateau in zone 2 as comprising SnO_2. Oxide film in this layer is not dense, likely discontinuous, and very thin. After completing the reduction process of oxide layers, the final plateau in zone 3 has undergone hydrogen evolution due to the reduction of the electrolyte. Figure 3(a) shows SERA curves obtained from oxidation of tin alloy in air at room temperature at various times. The widths of the initial potential drop, and the first and the second plateaus tend to increase as time passes. As illustrated in Figure 3(b), the potential drop in 72 h oxidation is the deepest of all tests, which means that clusters of oxide are growing, expanding, and converging to form a new continuous and uniform layer as time increases. The thickness of oxide films calculated from reduction current density [6] is shown in Table 1. It should be noted that the width of the first plateau decreases at the 24 h oxidation test, implying that the SnO film thickness shrinks. Other research [3,6,7] has stated that SnO can be transformed into the more stable SnO_2 over a longer time frame. The XPS data in the next section confirms this SnO to SnO_2 transformation phenomenon.

Figure 4 shows SERA curves obtained from oxidation of Sn-1 wt% Bi in deionized water at room temperature for various times. The results are similar to those of oxidation in air. There are three reduction zones. The thickness of oxide films tends to increase as the time passes. The oxide film thicknesses are greater than those observed in tests in air for all test times. Furthermore, it can clearly be seen that SnO layer thickness is reduced after 24 h, which is the same finding as in the 24 h oxidation test in air. The thickness of oxide films calculated from reduction current density is also shown in Table 2.

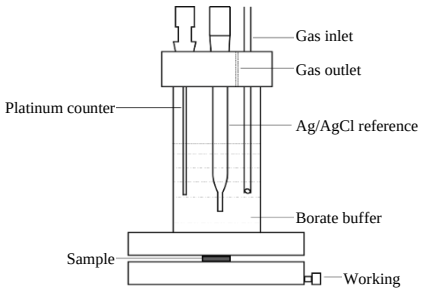

Figure 1. Schematic of electrochemical cell and separate compartments.

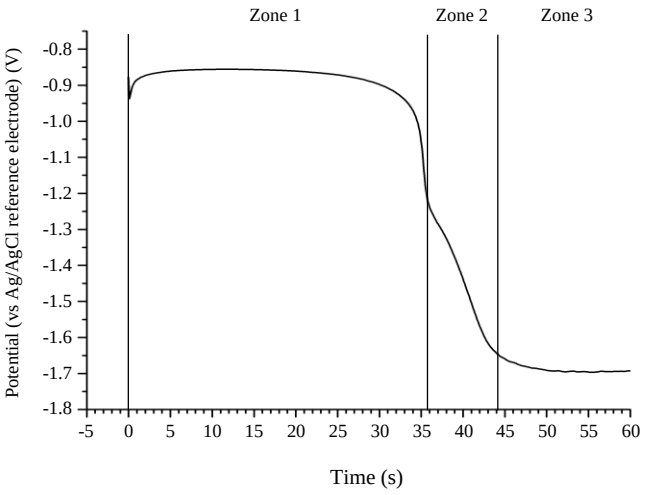

Figure 2. SERA curves obtained from oxidation of Sn-1 wt% Bi in air at room temperature for 72 h.

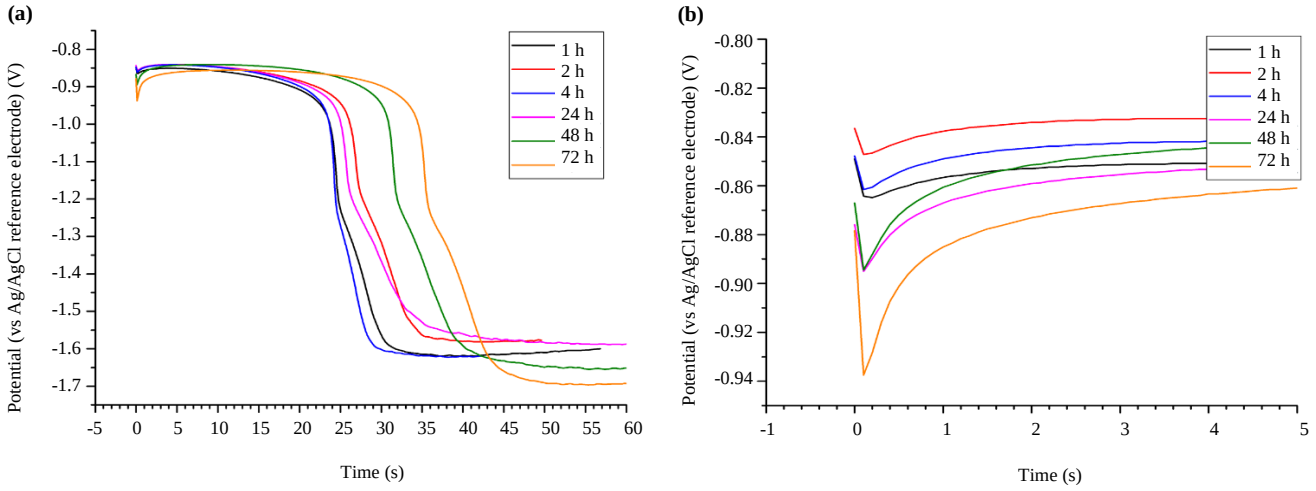

Figure 3. (a) SERA curves obtained for oxidation of Sn-1 wt% Bi in air at room temperature at various times and (b) the initial potential drop (color online).

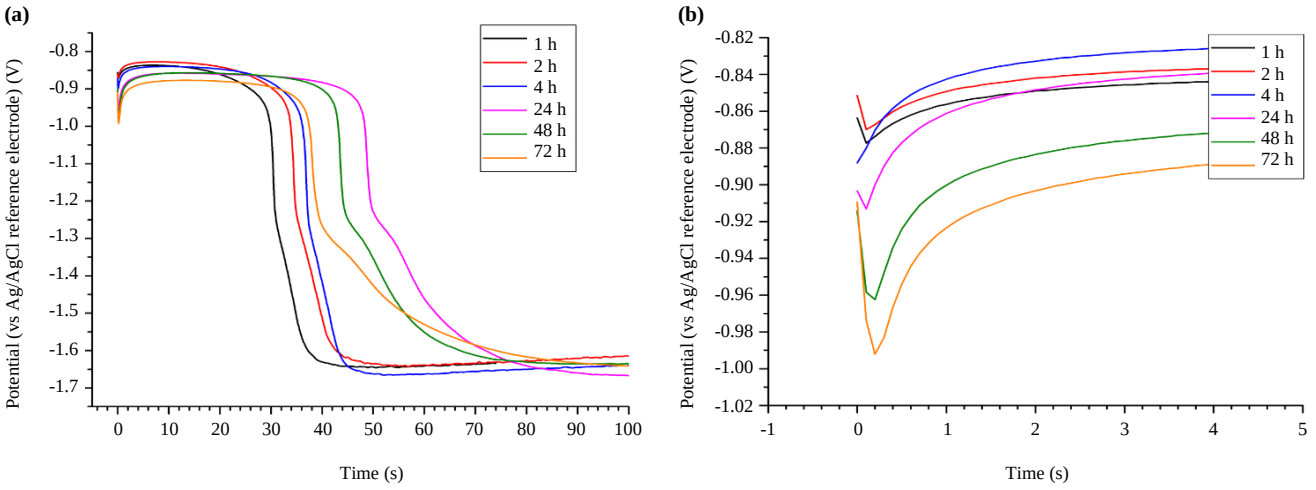

Figure 4. (a) SERA curves obtained for oxidation of Sn-1wt.%Bi in deionized water at room temperature at various times and (b) the initial potential drop (color online).

Table 1. Calculated thickness of oxide films for oxidation of Sn-1 wt % Bi in air at room temperature.

Time (h)	First plateau (Å)	Second plateau (Å)	Total thickness (Å)
1	14	1.5	15.5
2	14	1.5	15.5
4	15	1.3	16.3
24	14	1.7	15.7
48	18	2.4	20.4
72	21	2.5	24.0

Table 2. The thickness of oxide film for oxidation of tin alloy in deionized water at room temperature.

Time (h)	First plateau (Å)	Second plateau (Å)	Total thickness (Å)
1	18	2.4	20
2	19	2.8	21
4	22	2.9	25
24	30	4.4	34
48	24	5.6	30
72	24	8.6	33

Figures 5 and Figures 6 show plots of growth law of the oxide films. The relationship between film thickness and oxidation time, for both oxidation in air and deionized water at room temperature, can be described by a linear law for times shorter than 4 h which might be due to a discontinuous oxide layer [14,15]. It is followed by a parabolic growth law when the oxidation time is greater than 4 h. Thickness of oxide layer obtained from an oxidation in deionized water is noticeably greater than those obtained from an air-oxidation. It is suggested to be due to additional formation of tin hydroxide, which thereafter decomposes into more stable tin oxide [6,7]. The oxide growth laws found in this experiment are in good agreement with T. Tamai and Y. Nabeta tests in air for tin plated copper alloy [14,15]. Comparing the two plots in Figures 5 and Figures 6, it can be clearly seen that oxidation in deionized water occurs at a faster rate than oxidation in air. The results show that oxidation under deionized water is more severe than that in ambient atmosphere. After 72 h of oxidation (three days exposure), oxidation in air forms a 23 Å oxide layers, whereas oxidation in deionized water forms a 33 Å oxide layer.

3.2 Types of oxide film

X-ray photoelectron spectroscopy (XPS) was performed to determine the film composition on a sample surface. Figure 7 shows the effect of argon ion-beam etching a tin sample which was oxidized in air at room temperature. It reveals increasing intensity of Sn 3d5/2 peak when the etching time is increased. Deconvolution of these peaks, shown in Figure 8, specifies the type of Sn species, which implies the type of oxide formation. That is, Sn corresponds to metallic tin, Sn^{2+} corresponds to SnO, and Sn^{4+} corresponds to SnO_2. The peak positions of 3d5/2 for Sn, Sn^{2+}, and Sn^{4+} are 485.25 eV, 486.24 eV to 486.30 eV, and 487.00 eV to 487.05 eV, respectively [6,10-13]. Full width at half max (FWHM) of Sn, Sn^{2+}, Sn^{4+} peaks are 0.66, 1.8 and 1.3 eV, respectively. In Figure 8(b), the high intensity of the Sn^{4+} 3d5/2 peak indicates a dominance of SnO_2 at the outermost surface, which is in good agreement with the initial potential drop in zone 1 of the electrochemical analysis. Thus, the results suggest that a formation of thin and less-dense SnO_2 clusters is possible. As shown in Figure 8(c), after 150 s etching, the higher intensity of Sn^{2+} 3d5/2 and Sn^{0} 3d5/2 with a significant reduction of the intensity of Sn^{4+} 3d5/2 indicates removal of SnO_2 clusters by etching, revealing the underlying SnO and metallic tin. This is consistent with the SnO reduction plateau in zone 1 of the electrochemical analysis. In Figure 8(d), after 200 s etching, the intensity of Sn^{4+} 3d5/2 and Sn^{2+} 3d5/2 peaks are comparable, indicating a mixture of both SnO and SnO_2 at this depth, which is likely due to a transformation of SnO to SnO_2 underneath the SnO layer [3,6,7], exhibited as an obscure SnO_2 reduction plateau in zone 2 of the electrochemical analysis. The increased intensity of Sn 3d5/2, metallic tin, peaks in Figures 8(b-e) may be due to the preferential etching at asperities on the sample surface roughness. This preferential etching attack at asperity peaks exposes the Sn-1 wt% Bi substrate, and is detected by XPS at all etching times. Figure 9 summarizes the concentration of atomic species at each sputtering depth. After 300 s etching, oxygen concentration converges to zero, which indicates the end of the oxide film. According to the results, oxidation behavior of Sn-1 wt% Bi alloys at room temperature is found to be independent of the environment, being in air or deionized water, which is illustrated in Figure 10. The first layer consists of SnO_2 clusters. The second layer is a thick and continuous SnO layer. And the last, the third layer, is a mixture of SnO_2 and SnO compounds on top of the tin alloy substrate.

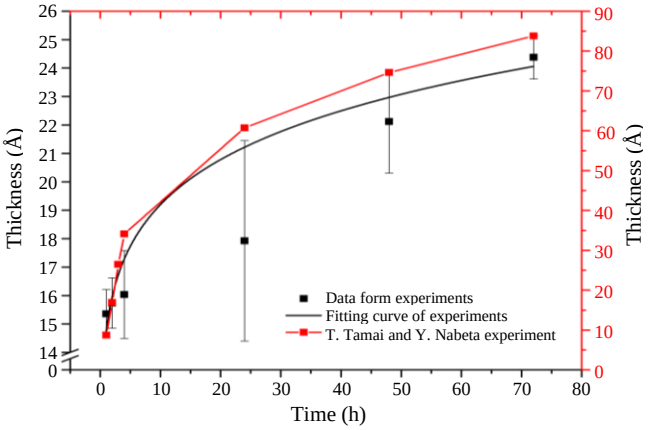

Figure 5. Thickness of oxide film versus oxidation time of tin alloy in air at room temperature [14,15] (color online).

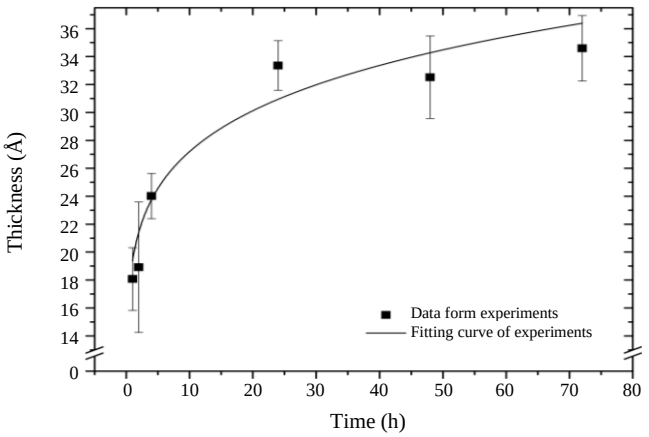

Figure 6. Thickness of oxide film versus time for oxidation of tin alloy in deionized water at room temperature.

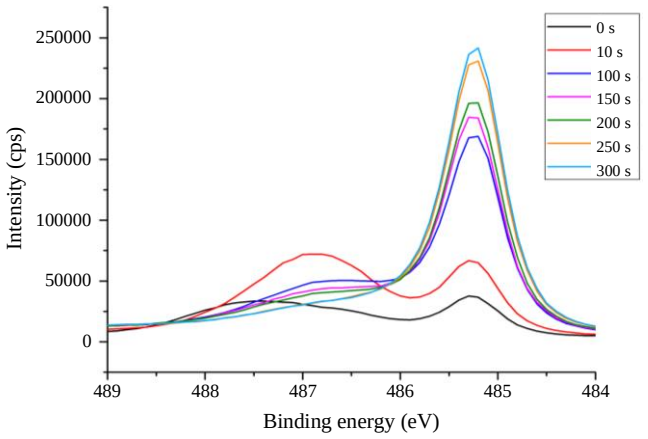

Figure 7. Effect of argon ion-beam etching on Sn 3d5/2 peak: 500 eV for 100 s (10 s per cycle), 1 keV for 100 s (10 s per cycle), and 3keV for 100 s (10 s per cycle), respectively (color online).

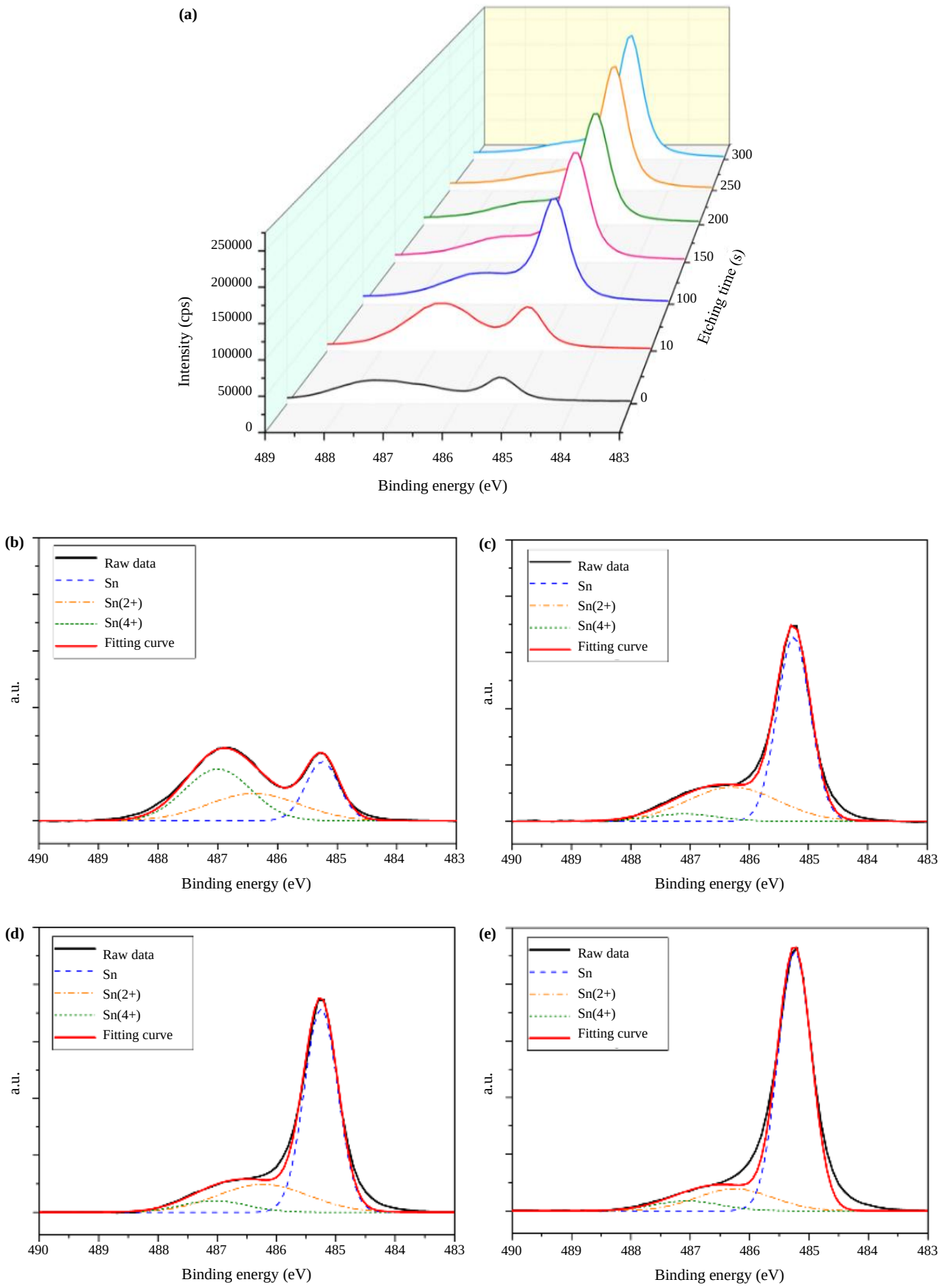

Figure 8. (a) Stack plots of XPS spectra for various etching times. Deconvoluted spectra of Sn 3d5/2 after (b) ion etching for 10 s, (c) ion etching for 150 s, (d) ion etching for 200 s, and (e) ion etching for 300 s (color online).

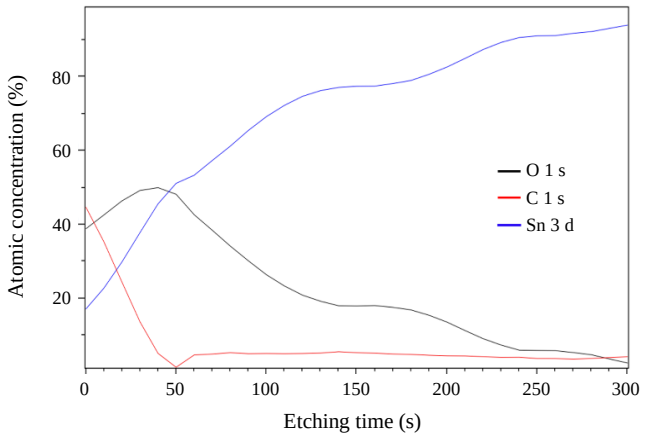

Figure 9. Concentration profiles of Sn, O and C with 500 eV for 100 sec (10 sec per cycle), 1 keV for 100 sec (10 sec per cycle), and 3keV for 100 sec (10 sec per cycle), respectively (color online).

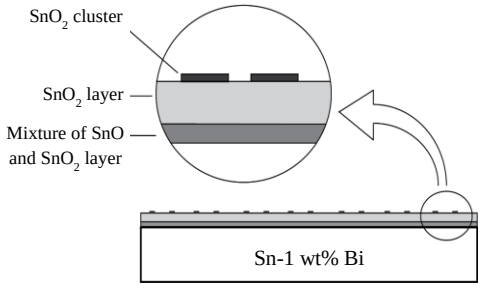

Figure 10. Schematic of oxides formation of Sn-1 wt% Bi in air and deionized water at room temperature (color online).

4. Conclusions

An investigation was conducted to evaluate and characterize oxidation of Sn-1 wt% Bi alloy in terms of oxide thickness and tin oxide species for two different conditions at room temperature. Tin alloy test samples were oxidized in air under a relative humidity of 30% to 32%, and in deionized water. Oxidation characteristics of both test conditions were the same. Two species of tin oxide were identified using the XPS technique, namely SnO (Tin(II)oxide; stannous oxide) and SnO_2 (Tin(IV)oxide; stannic oxide). Deconvolution of XPS spectra gave results corresponding well with those from electrochemical analysis. The results indicate SnO_2 is at the outermost surface, and may be in the form of clusters or a discontinuous thin layer, followed by a relatively thick and continuous SnO layer; the latter is the predominant species of the oxide film. The innermost layer is a mixture of the two oxides and cannot be well-defined. At room temperature, the growth of oxide film obeys early linear law behavior, and is then followed by a slower rate, which suggested parabolic law. After 72 h oxidation, the thickness of oxide films reaches 23 Å and 33 Å for tests in air and in deionized water, respectively.

Acknowledgements

The authors gratefully acknowledge Western Digital (Thailand) Co., Ltd. for the financial and materials support of the project.

References

[1] S. Kumar, and S. Suresh, "Study of photodegradation and wetting behavior on synthesis oxides of tin (stannous and stannic)," *Materialia*, no. 14, pp. 100869, 2020.

[2] A. F. James, "Tin-oxide thin films by thermal oxidation," M.S. thesis, Department of Phy. And Ast., Western Cape Univ., Bellville, April. 2021. Accessed on: August 9, 2021. [Online]. Available: https://etd.uwc.ac.za/handle/11394/8239

[3] D. M. Tench, M. W. Kendig, D. P.Anderson, D. D. Hillman, G. K. Lucey, and T. J. Gher, "Production Validation of SERA Solderability Test Method," *Solering & Surface Mount Technology*, no. 13, pp. 46-50, 1993.

[4] P. Bratin, M. Pavlov, G. Chalyt, and R. Gluzman, "New Application of the SERA Method Assessment of the Protective Effectiveness of Organic Solderability Preservatives," *Proceedings of the AESF annual technical conference*, vol. 82, pp. 583-590, 1995.

[5] D. T. Morgan, D. P. Anderson, and P. Kim, "Solderability assessment via sequential electrochemical reduction analysis," *Journal of Applied Electrochemistry*, vol. 24, no. 1, pp. 18-29, 1994.

[6] S. Cho, J. Yu, S.K. Kang, and D.Y. Shin, "Oxidation Study of Pure Tin and Its Alloys via Electrochemical Reduction Analysis" *Journal of Electronic Materials*, vol. 34, no. 5, pp. 635-642, 2005.

[7] D. D. Hillman, and L. S. Chumbley, "Characterization of tin oxidation products using sequential electrochemical reduction analysis (SERA)," *Soldering & Surface Mount Technology*, vol. 18, no. 3, pp. 31-41, 2006.

[8] S. Nakayama, T. Sugihara, T. Notoya, and T. Osakai, "Chemical State Analysis of Tin Oxide Films by Voltammetry reduction," *Journal of The Electrochemical Society*, vol. 158, no. 10, pp. C341-C345, 2011.

[9] B. Peter, P. Michael, and C. Gene, "Evaluating Finishes Using SERA" *PC FAB Magazine, May 1999*, 1999.

[10] C. L. Lau, and G. K. Wertheim, "Oxidation of tin: An ESCA study", *Journal of Vacuum Science & Technology*, vol. 15, no. 2, pp. 622-624, 1978.

[11] D. A. Asbury, and G. B. Hoflund, "A surface study of the oxidation of polycrystalline tin", *Journal of Vacuum Science & Technology A*, vol. 5, no. 4, pp. 1132-1135, 1987

[12] J. Luo, and C. Xu, "XPS Examination of Tin Oxide on Float Glass Surface" *Journal of Non-Crystalline Solids*, vol. 119, pp.37-40, 1990.

[13] B. V. Crist, "A Review of XPS Data-Banks" *XPS International LLC*, vol. 1, pp. 1-52, 2007.

[14] Y. Nabeta, Y. Saitoh, S. Sawada, Y. Hattori, and T. Tamami, "Growth Law of the Oxide Film Formed on the Tin Plated Contact Surface and Its Contact Resistance Characteristic", *2009 Proceedings of the 55th IEEE Holm Conference on Electrical Contacts*, pp. 176-181, 2009.

[15] T. Tamami, Y. Nabeta, S. Sawada, and Y. Hattori, "Property of Tin Oxide Film Formed on Tin-Plated Connector Contacts", 2010 Proceedings of the 56th IEEE Holm Conference on Electrical Contacts, pp. 1-8, 2010.